PHILOSOPHICAL TRANSACTIONS OF THE ROYAL SOCIETY A MATHEMATICAL, PHYSICAL & ENGINEERING SCIENCES

Lattice Boltzmann simulation of the flow of binary immiscible fluids with different viscosities using the Shan-Chen microscopic interaction model

Jonathan Chin

Phil. Trans. R. Soc. Lond. A 2002 **360**, 547-558
doi: 10.1098/rsta.2001.0953

10.1098/rsta.2001.0953

THE ROYAL SOCIETY

Lattice Boltzmann simulation of the flow of binary immiscible fluids with different viscosities using the Shan–Chen microscopic interaction model

By Jonathan Chin[1], Edo S. Boek[2] and Peter V. Coveney[1]

[1]*Centre for Computational Science, Queen Mary, University of London, London E1 4NS, UK* (j.chin@qmul.ac.uk)

[2]*Schlumberger Cambridge Research, High Cross, Madingley Road, Cambridge CB3 0EL, UK*
(boek@cambridge.scr.slb.com; p.v.coveney@qmul.ac.uk)

Published online 12 February 2002

We present a lattice Boltzmann study of the flow of a binary fluid where the fluid components have different viscosities. For this purpose, a microscopic interaction model (due to Shan & Chen) is used. The model is validated for Poiseuille flow of layered immiscible binary fluids and the dispersion of a capillary wave. We then study the unstable displacement of a viscous fluid by a less viscous fluid in a two-dimensional channel. Although a finger-like structure was observed in many simulations, it is not clear if this structure was produced due to viscous fingering or due to other effects.

Keywords: lattice Boltzmann simulation; viscous fingering; Shan–Chen microscopic interaction model

1. Introduction

If a less viscous fluid is forced into a more viscous one, the interface between the two fluids may become unstable: long fingers of the less viscous fluid penetrate into the bulk of the more viscous one, rather than evenly flushing it away. It was shown that the interface is unconditionally unstable in the absence of surface tension (Saffman & Taylor 1958), and that surface tension between immiscible fluids introduces a minimum wavelength for the instability. This instability is of considerable interest in, for example, the oil and oilfield services industry. A comprehensive review of the subject can be found in Homsy (1987).

The lattice Boltzmann equation (LBE) method may be regarded as a simplification of the lattice-gas automaton (LGA) or as a finite-difference method for solving the Boltzmann equation governing the evolution of the single-particle distribution function in a gas. It can be shown (by performing a Chapman–Enskog expansion) that, on macroscopic scales, both LGA (d'Humières *et al*. 1986) and LBE systems evolve according to the Navier–Stokes equations. Therefore, they provide a useful method for modelling fluid flow. Because no-slip boundaries are easily implemented, the method is particularly suited to simulate (multiphase) flow in complex geometries, such as porous media.

The LBE method was generalized by Gunstensen *et al.* (1991) for the simulation of two immiscible phases. A sharp interface between the two phases was obtained by phenomenological collision and recolouring rules. Flekkøy (1993) developed a multiphase miscible LBE scheme capable of modelling both the Navier–Stokes (N–S) and convection–diffusion (CD) equations in the one-phase region. Orlandini *et al.* (1995) introduced a multiphase LBE model designed to produce a well-defined isothermal equation of state. Here the equilibrium state minimizes a chosen free-energy function. The corresponding pressure tensor and chemical potential, coupling to the density difference, appear in the N–S and CD equations, respectively. This method is usually referred to as the Oxford model. It has the advantage that macroscopic parameters such as the surface tension can be supplied directly to the model (by choosing an appropriate form of the free energy).

Rakotomalala *et al.* (1997*a*, *b*) studied the displacement of miscible fluids of different viscosities (viscosity ratio M), as well as non-Newtonian fluid flow (Rakotomalala *et al.* 1996) between parallel plates. They used the LBE method, extending Flekkøy's (1993) model so that the components can have different viscosities. Above $M \sim 10$, the interface becomes a well-defined finger. At large M (they are able to achieve $M = 1000$ without getting instabilities), the reduced width tends to $\lambda = 0.56$. Langaas & Yeomans (1999) studied the displacement of binary immiscible fluids in a two-dimensional channel, using the 'thermodynamically consistent' Oxford model. The evolution of a single finger in a two-dimensional channel could be observed, producing results similar to those obtained experimentally by Saffman & Taylor (1958). For high viscosity ratios ($M \sim 100$), the finger width of the finger approached half the width of the channel.

In this paper, we will report a study of viscous fingering in two dimensions using the Shan–Chen (Shan & Chen 1994) binary immiscible fluid model, where the force term is related to the microscopic interactions between particles. This model will be described in the following section. Then the simulations will be discussed. First, the model is validated for Poiseuille flow of layered immiscible binary fluids and the dispersion of a capillary wave. Then we study the unstable displacement of a viscous fluid by a less viscous fluid in a two-dimensional channel.

2. Lattice Boltzmann method

We consider the LBE method as a preaveraged version of the LGA. Within this framework, fluids are represented by fictional particles with discrete velocities, occupying sites on a discrete lattice. In LGA, the occupation of each lattice site is restricted to an integer number of particles of each phase. The LBE method uses a real-valued single-particle distribution function, $f_i(\boldsymbol{x}) = f(\boldsymbol{x}, \boldsymbol{e}_i)$, defined for each lattice vector $\boldsymbol{e}_i$ at each site $\boldsymbol{x}$. The mass density $\rho(\boldsymbol{x})$ of single component σ at a given site $\boldsymbol{x}$ is, then,

$$\rho^\sigma(\boldsymbol{x}) = m^\sigma \sum_i f_i^\sigma(\boldsymbol{x}). \tag{2.1}$$

The momentum of single component σ is given by

$$\rho^\sigma \boldsymbol{u}^\sigma = m^\sigma \sum_i f_i^\sigma \boldsymbol{e}_i, \tag{2.2}$$

where $\boldsymbol{u}$ is the mean particle velocity. The simulations described here use two components, called 'red' and 'blue', to represent oil and water.

In order to capture fluid dynamics, the distribution function is manipulated by an advection–collision process for each time-step. The values of the distribution function are advected along their velocity vectors, and then a new distribution function is calculated at each site to represent the effect of collision:

$$f_i^\sigma(\boldsymbol{x}+\boldsymbol{e}_i, t+1) = f_i^\sigma(\boldsymbol{x}, t) + \Omega_i^\sigma, \tag{2.3}$$

where Ω_i^σ is the collision term. It must be chosen in such a way as to conserve the total mass of each phase at each site and to conserve the total momentum at each site, i.e.

$$\sum_i m^\sigma \Omega_i^\sigma = 0, \tag{2.4}$$

$$\sum_i \sum_\sigma m^\sigma \Omega_i^\sigma \boldsymbol{e}_i = 0. \tag{2.5}$$

The operator used here is known as the Bhatnagar–Gross–Krook (or BGK) operator. The distribution of particles at equilibrium, $f_i^{\sigma(\mathrm{eq})}$, is determined, and the rate at which the particle distribution relaxes to equilibrium is controlled by a time τ^σ; hence

$$\Omega_i^\sigma = -\frac{1}{\tau^\sigma}(f_i^\sigma - f_i^{\sigma(\mathrm{eq})})$$

and, therefore,

$$f_i^\sigma(\boldsymbol{x}+\boldsymbol{e}_i, t+1) - f_i^\sigma(\boldsymbol{x}, t) = -\frac{1}{\tau^\sigma}(f_i^\sigma - f_i^{\sigma(\mathrm{eq})}). \tag{2.6}$$

It has been shown (Qian *et al*. 1992) that a suitable choice of equilibrium distribution leads to the reproduction of Navier–Stokes hydrodynamics on sufficiently coarse length-scales. The equilibrium distribution is a function only of number density $n = \rho/m$ and velocity $\boldsymbol{u}$ of particles at a site:

$$f_i^{\sigma(\mathrm{eq})} = nT_i\left[1 + \frac{e_{i\alpha}u_\alpha}{c_\mathrm{s}^2} + \frac{u_\alpha u_\beta}{2c_\mathrm{s}^2}\left(\frac{e_{i\alpha}e_{i\beta}}{c_\mathrm{s}^2} - \delta_{\alpha\beta},\right)\right], \tag{2.7}$$

where the weighing factors T_i are chosen to ensure isotropic hydrodynamics and c_s^2 is the speed of sound (which depends only on the lattice).

(*a*) *The Shan–Chen model*

We use the Shan–Chen generalization of the lattice BGK model for multicomponent fluids with interactions (Shan & Chen 1993). In this model the equilibrium distribution (2.7) is retained but a different velocity $\boldsymbol{v}^\sigma$ is used for each component. It was assumed that, during each collision step, the velocities of each different phase quickly equalize in the absence of forces. The velocity $\boldsymbol{v}^\sigma$ of component σ is perturbed to take account of collisions with other components as well as a small increment due to the force $\boldsymbol{F}^\sigma$ acting on that component:

$$\boldsymbol{v}^\sigma = \left[\left(\sum_\sigma \frac{\rho^\sigma}{\tau^\sigma}\boldsymbol{u}^\sigma\right)\Big/\left(\sum_\sigma \frac{\rho^\sigma}{\tau^\sigma}\right)\right] + \frac{\rho^\sigma}{\tau^\sigma}\boldsymbol{F}^\sigma. \tag{2.8}$$

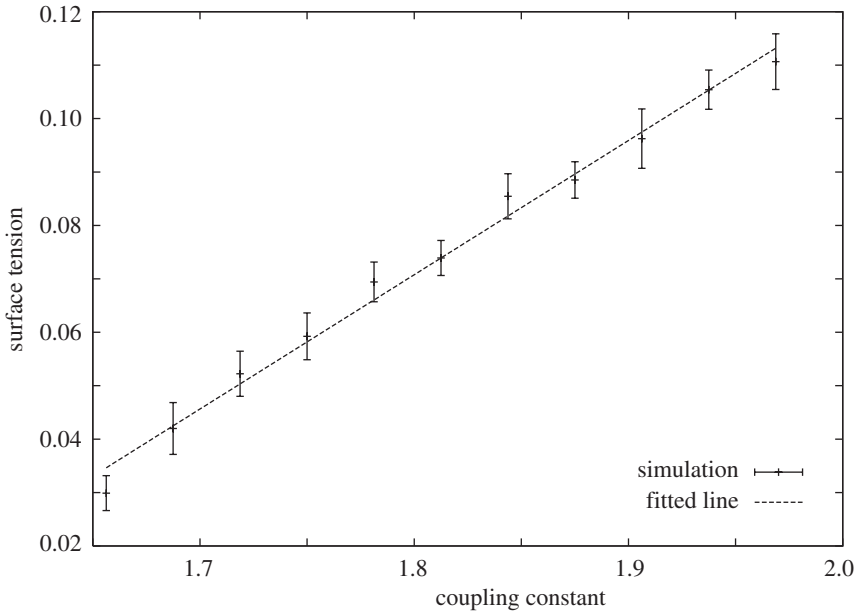

Figure 1. Surface tension versus coupling constant for $\tau_r = \tau_b = 1.0$. The error bars indicate the error in surface tension derived from fitting a Laplace law relationship to each simulation set at a single value of the coupling parameter.

The force $\boldsymbol{F}^\sigma$ includes a gravitational force acting in the z-direction ($G\rho^\sigma \hat{\boldsymbol{z}}$) and an immiscibility force to bring about separation of phases. The model proposed by Shan & Chen (1993) has a nearest-neighbour interaction between different phases σ and $\bar{\sigma}$, controlled by a coupling constant $g_{\sigma\bar{\sigma}}$, so that the full force $\boldsymbol{F}^\sigma$ reads

$$\boldsymbol{F}^\sigma(\boldsymbol{x}) = -g_{\sigma\bar{\sigma}}\psi^\sigma(\boldsymbol{x})\sum_i \psi^\sigma(\boldsymbol{x}+\boldsymbol{e}_i)\boldsymbol{e}_i + G\rho^\sigma\hat{\boldsymbol{z}}. \tag{2.9}$$

In order to model immiscible fluids, ψ^σ may simply be set to ρ^σ; $g_{\sigma\bar{\sigma}}$ is set to zero for $\sigma = \bar{\sigma}$, and a positive value for $\sigma \neq \bar{\sigma}$: for a given component, this will produce a force in a direction directly away from any interfaces. The coupling constant $g_{\sigma\bar{\sigma}}$ is vaguely analogous to the variable κ in the model of Orlandini *et al.* (1995) insofar as larger values give rise to larger surface tensions. However, the surface tension simulated is a function of both the coupling constant and the relaxation times of the components. While expressions exist (Shan & Chen 1993) for the surface tension in a liquid–gas Shan–Chen model as a function of simulation parameters, currently the surface tension of a multicomponent fluid model must be found through simulation. In general, the surface tension increases with increasing coupling constant and decreasing relaxation times.

A brief examination using the Laplace law relationship between the pressure drop across the interface of a bubble and its radius suggests an almost linear relationship between the surface tension and coupling constant, as can be seen in figure 1.

(*b*) *'Top-down' versus 'bottom-up'*

The Oxford model is often referred to as a 'top-down' LBE model, since it imposes a macroscopic free-energy functional. The Shan–Chen model, on the other hand,

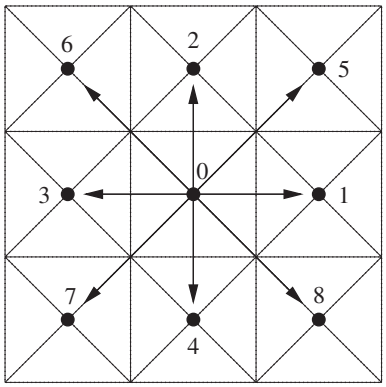

Figure 2. The D2Q9 lattice.

is a phenomenological 'bottom-up' model, since the force term (2.9) is related to microscopic interactions between particles. It may be considered as an advantage of the top-down model that macroscopic parameters (such as surface tension) can be chosen and supplied directly to the model. However, it is not evident that minimizing a free-energy functional, valid in thermodynamic equilibrium, is appropriate when studying a non-equilibrium dynamics problem such as fluid flow. Moreover, in the absence of any guarantee, such as an H-theorem, that an equilibrium state will always be reached, it is not clear how much weight arguments about equilibrium dynamics should carry. It should additionally be noted that imposing a free-energy functional will produce models that give no information about how microscopic interactions produce such a free energy in the first place.

(*c*) *The two-dimensional D2Q9 lattice*

We use a two-dimensional LBE implementation with the three-speed D2Q9 lattice, which consists of a null vector for particles at rest, four vectors of unit length in the Cartesian directions, and four vectors of length $\sqrt{2}$ in the diagonal directions (figure 2).

(*d*) *Viscosity in lattice Boltzmann*

It has been shown (Qian *et al*. 1992) that for the D2Q9 lattice, the viscosity of a single pure phase is a function only of its relaxation time:

$$\nu = \tfrac{1}{3}(\tau - \tfrac{1}{2}). \tag{2.10}$$

The viscosity of a mixture of two fluids (red and blue) is given by Shan & Doolen (1995):

$$\nu = \tfrac{1}{3}x_{\mathrm{r}}(\tau_{\mathrm{r}} - \tfrac{1}{2}) + \tfrac{1}{3}x_{\mathrm{b}}(\tau_{\mathrm{b}} - \tfrac{1}{2}), \tag{2.11}$$

where x_{r} and x_{b} are the fractions of red and blue, respectively, and τ_{r}, τ_{b} are the relaxation times for red and blue. By choosing relative relaxation times, viscosity ratios up to 10 can be achieved.

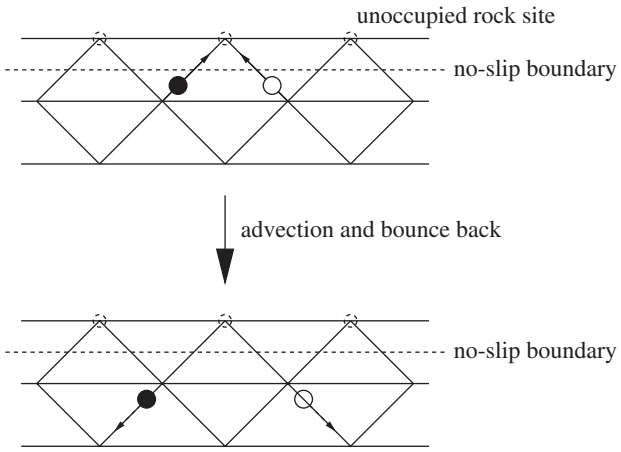

Figure 3. The reflection of particles along the direction from which they came results in a 'no-slip' boundary condition.

(*e*) *Boundary conditions in the LBE model*

The presence of obstacles or walls obeying 'no-slip' boundary conditions can be simulated through the use of 'bounce-back' sites on the lattice. This makes LB ideal for explicit simulation of fluid flow in complex geometries, such as porous media. The bounce-back sites do not contain any fluid particles, and when particles advect in to such sites, their velocity vectors are reversed (figure 3). Note that the position of the boundary is actually located halfway between the obstacle sites and the adjacent lattice sites.

(*f*) *Lattice Boltzmann versus lattice gas*

The chief advantage of the lattice Boltzmann method over lattice gas is that it requires substantially less computation to model a given phenomenon, due to the comparative noisiness of the lattice-gas method; the chief advantage of lattice gas over lattice Boltzmann is its unconditional stability. In addition, lattice-gas models suffer from a lack of Galilean invariance, which may be remedied for single-phase models through the use of a scaling technique.

The lattice Boltzmann model is deterministic, in contrast to the stochastic lattice-gas method. This means that kinetic fluctuations are not present, which affects the accessible phenomenology. For example, it has been suggested (Chen *et al*. 2001) that the reason lamellar structures (in multiphase fluids involving surfactants) are easily found in two-dimensional LBE models, but not observed in two-dimensional LGA models, is that the Peierls instability prohibits their existence in models with fluctuations.

The main disadvantage of the lattice Boltzmann model is that numerical instabilities may arise, which severely limit the range of parameters to the model. The reason for this is that no H-theorem has been proved for an interacting lattice BGK model, which means that the algorithm is not unconditionally stable. Indeed, in a study of interfacial dynamics in three-dimensional binary fluids (Pagonabarraga *et al*. 2001), the Oxford LBE model is reported to become unconditionally unstable, that is all simulations eventually become unstable when left running. We observe

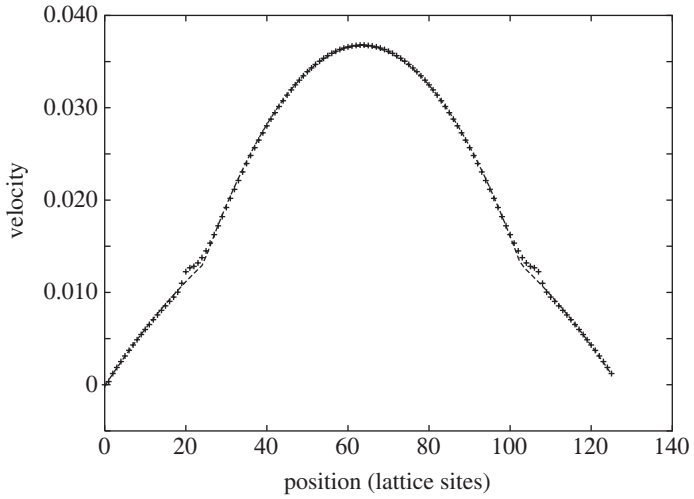

Figure 4. Simulated and analytical velocity profiles (simulated, +; analytical, – – –).

that, using the Shan–Chen model, numerical instabilities occur when the viscosity ratio $M > \mathcal{O}(10)$. However, every simulation that is stable for the first 100–1000 time-steps remains so unless the way of forcing is changed, or one keeps adding momentum to the system.

3. Results and discussion

We test the model by considering simple flows for which analytical results are available. Note that these analytical results are for two-phase flow with a sharp interface. Our simulations on the other hand have a finite interface width.

If a linear interface is simulated with a coupling constant $g_{\sigma\bar{\sigma}} = 2.0$ and relaxation time $\tau = 1.0$ for both components, the distance between the point where the red component reaches 98% of its maximum density and the point where the blue component reaches 98% of its maximum density is about 10 lattice spacings. This interface width decreases with increasing coupling constant $g_{\sigma\bar{\sigma}}$. Thus the LB method is suitable for simulating two-phase problems on a *mesoscopic* scale, where a finite interface width is important.

The finite interface width can obscure matters somewhat when measurements of the interface position are required, for example, when tracking the motion and shape of a capillary wave or viscous finger. In these studies, we follow the convention of defining the interface position to be at the point where the red and blue particle densities are equal. For situations where an appreciable amount of mixing of the two components occurs over a wide interfacial region, this places the interface position very near to the centre of the mixing region between the two bulk phases.

(*a*) *Poiseuille flow*

Consider a two-dimensional channel with non-slip boundaries at $x = \pm L$, filled with a fluid of viscosity ν_i in the region $0 < |x| < a$, and another fluid of viscosity ν_o in the region $a < |x| < L$. If a body force G is applied in the y-direction, the Navier–Stokes equations may easily be solved to give the y-velocity in the channel.

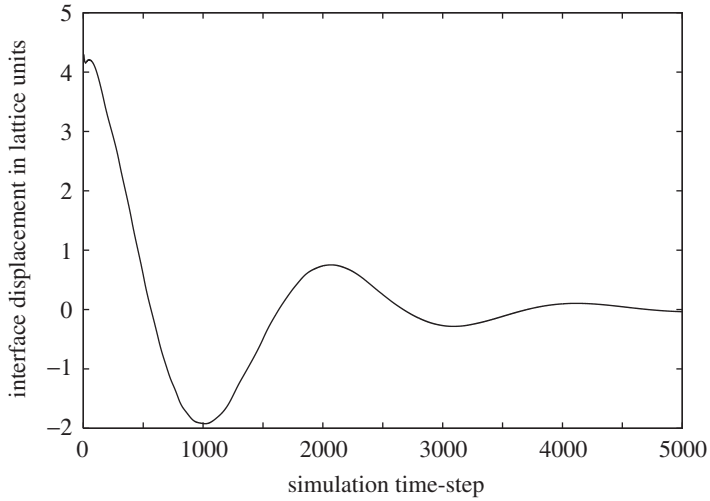

Figure 5. The y-position of the interface in a capillary wave plotted against time.

For $a < |x| < L$,

$$u(x) = \frac{G}{2\nu_o}(L^2 - x^2). \tag{3.1}$$

For $0 < |x| < a$,

$$u(x) = \frac{G}{2\nu_o}(L^2 - a^2) + \frac{G}{2\nu_i}(a^2 - x^2). \tag{3.2}$$

Simulations were initialized with a region of low-viscosity ($\tau = 1.0$) component, of width $2a$ lying between regions of high-viscosity ($\tau = 3.0$) component. Periodic boundary conditions were imposed at the y-boundaries. Initially, both fluids had zero velocity; the system was allowed to equilibrate, and then the velocity profile was measured. As can be seen from figure 4, the results match the analytical result closely, away from the interface.

(*b*) *Capillary wave dispersion*

Following the procedure of Langaas & Yeomans (1999), we simulate the decay in amplitude of a capillary wave. The system is periodic in the x-direction, and non-slip boundaries are imposed at $y = \pm L$. The region $y > 0$ is filled with the red component, and the $y < 0$ region filled with the blue component; the interface is initially set to be a sinusoidal curve of wavelength λ such that $2L = m\lambda$ for integer m, ensuring that an integer number of wavelengths exactly fits the width of the simulation. The interface is then permitted to relax, producing a damped capillary wave.

At every time-step of the simulation, the position of the interface at $x = L - \lambda/4$ is noted; as can be seen from figure 5, an exponentially decaying wave results. The frequency ω of the wave was measured as a function of wave-vector k, and, in agreement with the results of Langaas & Yeomans (1999), the dispersion relation fits a power-law curve of the form $\omega = Ak^{3/2}$, as can be seen in figure 6.

This relation can also provide a dynamical measurement of surface tension, as opposed to the measurement of static surface tension from Laplace law studies. The

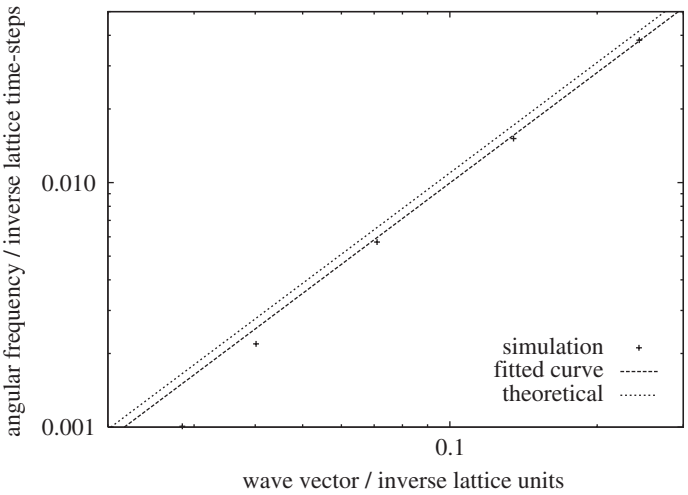

Figure 6. The frequency ω of capillary waves against wave-vector k, along with a fitted power law, and the expected analytical behaviour.

capillary wave measurements suggested a surface tension of 0.09, a slightly lower value than the 0.12 determined from the Laplace law studies.

(*c*) *Viscous fingering in two dimensions*

We use the Shan–Chen LB model to study viscous fingering in two dimensions. The system studied is a two-dimensional channel, with bounce-back walls on either side. Initially, the system only contains red particles, and incoming particles are assigned the colour blue. To avoid boundary effects, a Poiseuille distribution is used for the in/out velocities. This produces a pressure gradient driving the flow.

The driving fluid should produce a finger if the viscosity ratio

$$M = \frac{\nu_1}{\nu_2} = \frac{\tau_\mathrm{r} - \frac{1}{2}}{\tau_\mathrm{b} - \frac{1}{2}} \tag{3.3}$$

is large enough. An additional requirement is that the capillary number

$$\mathrm{Ca} = un\nu/\sigma \tag{3.4}$$

is also large enough, where u is the velocity of the tip of the finger, n is the number density of particles, and ν is the higher viscosity. In the simulations described below, u was typically of order 0.1, $n = 2.0$, $\nu = 1.3$; the surface tension σ was at most of order 0.1, giving Ca of order unity or larger. The coupling constant was varied between 1.0 and 1.8. We will be presenting results for $1.0 \leqslant \tau_\mathrm{r} \leqslant 4.0$, keeping τ_b fixed at a value of 1.0. This corresponds to viscosity ratios varying between 1 and 7. Numerical instabilities occur for $\tau_\mathrm{r} > 4$, which means that significantly higher viscosity ratios currently cannot be achieved.

The time evolution of the interface between the two phases, defined as the region where the particle densities of each fluid are equal, is shown for various time-steps and simulation parameters in figure 7.

We start with a flat interface, and a clear finger-like structure develops in all cases. A number of observations can be made from this figure. First of all, the finger

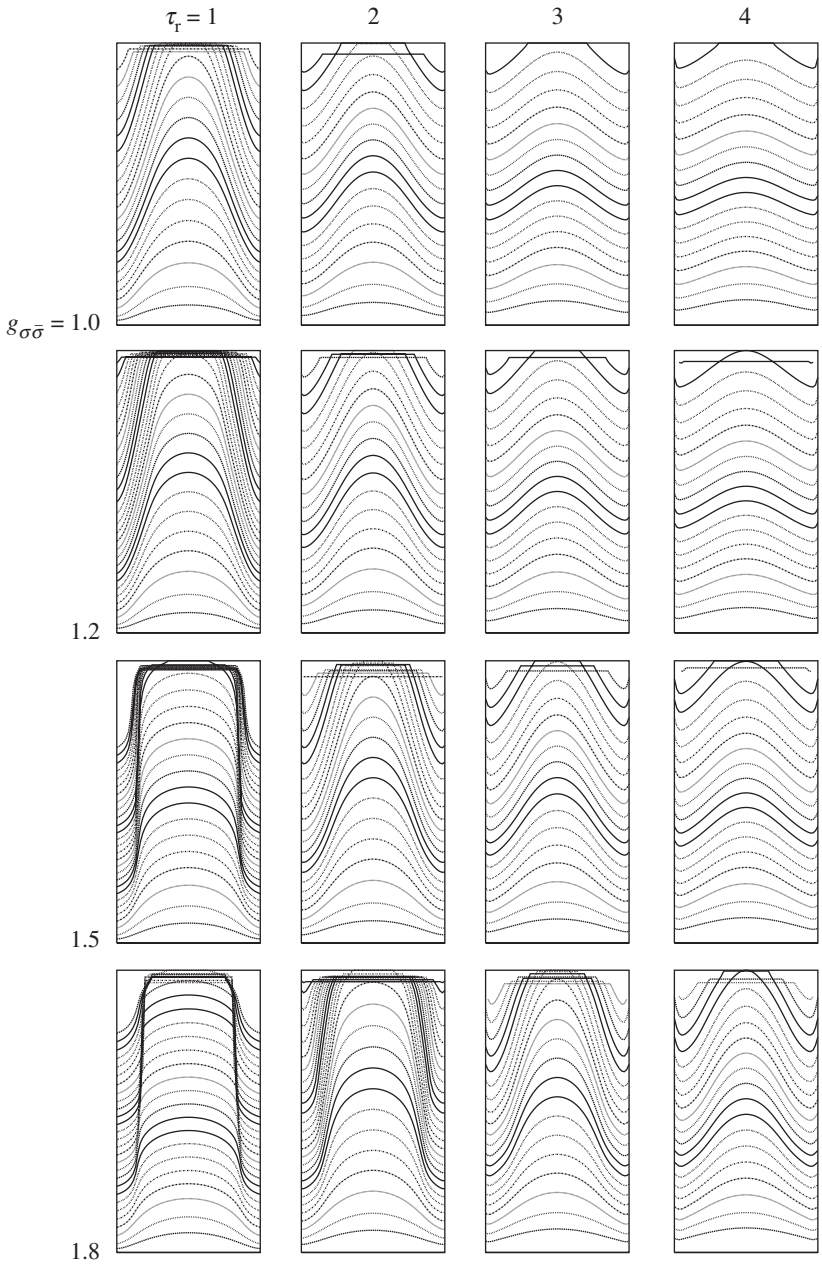

Figure 7. The time evolution of the fluid interface, plotted every 250 time-steps for different coupling constants and relaxation times. Each box is 64 lattice sites wide and 256 lattice sites long.

width appears to increase with increasing surface tension, for low viscosity ratios, in agreement with the observations of Langaas & Yeomans (1999).

Unfortunately, this effect is unclear for higher viscosity ratios, possibly due to the tendency of the components to mix more when the viscosity is increased: for

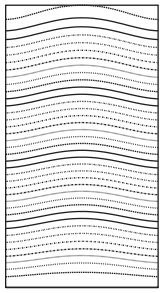

Figure 8. The time evolution of the fluid interface plotted every 250 time-steps for infinite capillary number at a 1 : 7 viscosity ratio. The simulation box is 64 lattice sites wide and 256 lattice sites long.

$g_{\sigma\bar{\sigma}} = 1.0$, the interface width varies from around 5–10 sites at $\tau_r = 1.0$ to 40 or more sites at $\tau_r = 4.0$. This tendency to mix is because the diffusivity of each component, as well as its viscosity, increases as its relaxation time is increased.

Secondly, the development of a finger is more clear in simulations at higher surface tensions, which is counterintuitive: one would normally expect an increased surface tension to make the production of finger-like structures less favourable.

Third, the interface for zero surface tension (and therefore infinite capillary number) at a 1 : 7 viscosity ratio, shown in figure 8, appears to be almost flat, although the components are highly mixed. It is possible that the effect of increased miscibility is competing with any viscous instability effects, obscuring the development of fingers at higher viscosity ratios.

4. Summary

A lattice Boltzmann model of the flow of binary immiscible fluids with different viscosities, using the Shan–Chen interaction model, has been developed to study viscous fingering in two dimensions. The model is suitable for simulation of two-phase flow on the mesoscopic scale, where the finite width of the fluid interface is important. Under some regimes, the limit of zero interface width may be difficult to probe. The reason is that the width is reduced by increasing the coupling parameter, which reduces the stability of the code. The model was first used to study Poiseuille flow in a two-dimensional channel. Good agreement with the analytic solution (for zero interface thickness) was obtained. Then the model was used to simulate the displacement of a fluid by a less viscous one in a two-dimensional channel. A viscous-fingering-like phenomenology was observed for viscosity ratios M up to $\mathcal{O}(10)$. For larger viscosity ratios, the Shan–Chen LBE algorithm becomes unstable. The fingers were also seen to be more pronounced for systems with high surface tension: this suggests that the mechanism producing the finger-like shapes may not be viscous fingering.

References

Chen, H., Boghosian, B. M., Coveney, P. V. & Nekovee, M. 2001 A lattice Boltzmann model of ternary amphiphilic fluids. *Proc. R. Soc. Lond.* A **456**, 2043.

d'Humières, D., Lallemand, P. & Frisch, U. 1986 Lattice gas model for 3D hydrodynamics. *Europhys. Lett.* **2**, 291–297.

Flekkøy, E. G. 1993 Lattice Bhatnagar–Gross–Krook models for miscible fluids. *Phys. Rev.* E **47**, 4247–4257.

Gunstensen, A. K., Rothman, D. H., Zaleski, S. & Zanetti, G. 1991 Lattice Boltzmann model of immiscible fluids. *Phys. Rev.* A **43**, 4320–4327.

Homsy, G. M. 1987 Viscous fingering in porous media. *A. Rev. Fluid Mech.* **19**, 271–311.

Langaas, K. & Yeomans, J. M. 1999 Lattice Boltzmann simulation of a binary fluid with different phase viscosities and its application to fingering in two dimensions. *Eur. Phys. J.* B **15**, 133–141.

Orlandini, E., Swift, M. R. & Yeomans, J. M. 1995 A lattice Boltzmann model of binary-fluid mixtures. *Europhys. Lett.* **32**, 463–468.

Pagonabarraga, I., Desplat, J.-C., Wagner, A. J. & Cates, M. E. 2001 Interfacial dynamics in 3D binary fluid demixing: animation studies. *New J. Phys.* **3**, 9.1–9.18.

Qian, Y. H., d'Humières, D. & Lallemand, P. 1992 Lattice BGK models for Navier–Stokes equation. *Europhys. Lett.* **17**, 479–484.

Rakotomalala, N., Salin, D. & Watzky, P. 1996 Simulations of viscous flows of complex fluids with a BGK lattice gas. *Phys. Fluids* **8**, 3200–3202.

Rakotomalala, N., Salin, D. & Watzky, P. 1997*a* Fingering in 2D parallel viscous flow. *J. Phys. France* **7**, 967–972.

Rakotomalala, N., Salin, D. & Watzky, P. 1997*b* Miscible displacement between two parallel plates: BGK lattice simulations. *J. Fluid Mech.* **338**, 277–297.

Saffman, P. G. & Taylor, G. I. 1958 The penetration of a fluid into a porous medium or Hele–Shaw cell containing a more viscous liquid. *Proc. R. Soc. Lond.* A **245**, 312–329.

Shan, X. & Chen, H. 1993 Lattice Boltzmann model for simulating flows with multiple phases and components. *Phys. Rev.* E **47**, 1815–1819.

Shan, X. & Chen, H. 1994 Simulation of nonideal gases and liquid–gas phase transitions by the lattice Boltzmann equation. *Phys. Rev.* E **49**, 2941–2948.

Shan, X. & Doolen, G. 1995 Multicomponent lattice Boltzmann model with interparticle interaction. *J. Stat. Phys.* **81**, 379–393.